Materials Science & Engineering A 897 (2024) 146358

Contents lists available at ScienceDirect

Materials Science & Engineering A

journal homepage: www.elsevier.com/locate/msea

Work hardening of quaternary powder metallurgy Ti alloys

M. Al-hajiri, F. Yang, L. Bolzoni *

School of Engineering, The University of Waikato, Hamilton, 3240, New Zealand

ARTICLE INFO

Keywords:
Titanium alloys
Powder metallurgy
Blended elemental
Homogeneous microstructure
Mechanical properties

ABSTRACT

The concurrent addition of Al as α stabiliser and Nb and Cu or Mn as β stabilisers was used to design new powder metallurgy quaternary Ti alloys and investigate their manufacturability and consequent performance. It is found that the powder blend's compressibility decreases with the total amount of alloying elements due to the characteristics of the powders used. Consequently, the sintered density of the quaternary Ti alloys decreases and slightly higher values are achieved if Mn instead of Cu is used, despite the higher diffusivity of Cu at the sintering temperature. The quaternary Ti alloys are characterised by a lamellar microstructure comprising α grain boundaries and α+β lamellae where the amount and type of alloying elements determine the coarseness of the microstructural features. This results in stronger and harder but less ductile quaternary Ti alloys for higher alloying elements contents and for stronger β stabilisers, although of their overall elastoplastic behaviour. Because of their lamellar microstructure, the quaternary Ti alloys show similar deformation behaviour but the actual work hardening rate is governed by the fineness of the microstructure.

1. Introduction

Ti is a relatively new engineering material as compared to other structural metals [1] and has primarily caught the attention of high demanding sectors including aerospace, petrochemical, and biomedical [2]. This is due to two competing factors, namely its cost and its combination of properties. On the one side, Ti is expensive to extract due to its high affinity for oxygen making its extractive metallurgy challenging and costly as high energy intensive. On the other side, Ti is lightweight, strong, biocompatible and corrosion resistant in many aggressive environments. Ti is also characterised by allotropy as it crystallises into a hexagonal structure at room temperature (known as α Ti) which transforms into a body centred cubic lattice (known as β) once the allotropic phase transformation β transus is crossed. Alloying elements added to Ti are, therefore, classified as neutral, α stabilisers or β stabilisers depending on which phase they contribute to stabilise where the latter stabilisers are also divided into isomorphous and eutectoid depending on their maximum solubility [3,4]. The addition of different alloying elements can result in a Ti alloy being composed of only a stable phase (i.e. α or β) or a combination of the two, leading to α, α+β, and β Ti alloys, respectively [5–7]. For developing new α+β Ti alloys, which are the one with the best strength/ductility compromise, Al is generally the α stabiliser of choice [8] as it decreases the density of the alloy, it improves strength, deformability and corrosion resistance, and it is cheap and readily available. In terms of β stabilisers, different elements are added for several purposes like their β stabilisation power, enhance processability and performance, and achieve specific functionalities [9–11]. Amongst β stabilisers, Nb, Cu, and Mn are primarily considered for enhancing biocompatibility, obtain antibacterial capability, and improve mechanical properties, respectively.

Literature shows that comprehensive understanding of the addition of Nb, Cu, and Mn in the respective binary alloys has been generated. The number of studied considering the manufacturing of binary alloys via casting is extensive whilst is much more limited in the case of powder metallurgy. For instance, the effects that different Nb contents (i.e. 5-45% for cast alloys [12–16] and ≥10% for powder metallurgy alloys [17–19]; compositions are in percentage by weight unless otherwise indicated) have on the microstructure and resulting properties is readily available. Main highlights are that the addition of Nb increases corrosion resistance as well as cell and mitochondrial proliferation as proved, after 7 days of exposure to, respectively, MC3T3-E1 and GM7373 cells [20]. Moreover, promising L929 and MG-63 cells attachment, proliferation, and differentiation was found in cytotoxic evaluations [16]. With regard to binary Ti–Cu alloys, Cu contents of 0.5–10% [21–24] in the case of casting and 2–25% in the case of vacuum hot pressure sintering [25,26] have been analysed. It was found that the addition of Cu brings about superior capability to inhibit bone resorption due to bacterial infection, as tested with *E. coli* and *S. aureus* bacterial colonies,

* Corresponding author.
E-mail address: bolzoni.leandro@gmail.com (L. Bolzoni).

https://doi.org/10.1016/j.msea.2024.146358
Received 3 December 2023; Received in revised form 3 March 2024; Accepted 9 March 2024
Available online 11 March 2024

combined with restrained formation of biofilms without affecting the corrosion resistance. Similarly, the effects of different Mn contents (i.e. 5-20% for cast alloys [27–31] and 1–17% for powder metallurgy alloys [32,33]) has been analysed in the case of binary Ti–Mn alloys. The key finding is related to the fact that prevention of Mn intoxication and of the precipitation of the brittle metastable ω phase is achieved if the amount of Mn is kept below 8%.

When it comes to ternary alloys, literature shows that the number of studies that analysed the manufacturing and properties of alloys entailing the concurrent addition of two of the previously mentioned alloying elements (i.e. Al, Nb, Cu or Mn) is much more limited. The most classical example of the simultaneous addition of Al and Nb is obviously the Ti–6Al–7Nb alloy, which was developed as part of the second generation of biomedical Ti alloys replacing V due to its cytotoxicity. A wider range of Al and Nb combinations has been studied by Matlakhova et al. [34] showing that the elastic modulus increases with the Al and decreases with the Nb percentage due to different developed structures, especially at lower Al contents. In the case of ternary Ti–Al–Cu alloys, examples are the work of Koike et al. [35] who developed cast Ti–5Al–Cu alloys for dental applications, and Sherif et al. [36] who analysed induction sintering as an alternative manufacturing technique for these alloys and quantified their corrosion resistance. Regarding the Ti–Al–Mn system, Blacha et al. [37] and Mikhaylovskaya et al. [38], respectively, analysed the change in composition during smelting in a vacuum induction furnace and the superplastic behaviour of a near-α alloy, but no mechanical properties were quantified. Concerning ternary Ti–Nb–Cu alloys, Takahashi et al. [39] studied the microstructure and mechanical properties of cast Ti-(6–24)Nb-(1–4)Cu alloys for dental applications, whereas Mutlu and Oktay quantified the corrosion behaviour of Ti–35Nb-(3–10)Cu alloys [40]. Around the ternary Ti–Nb–Mn system, Chen et al. [41] manufactured Ti–27Nb-(0–9%) Mn alloys via casting whilst Ehtemam-Haghighi et al. [42] considered Ti–7Mn-(3–10)Nb alloys (x = 3–10%) obtained via powder metallurgy. Lastly, the main research performed on ternary Ti–Cu–Mn alloys [43,44] was carried out by the authors of the current work to quantify the antibacterial capability of such alloys.

Literature, therefore, shows that the scientific knowledge developed on respective ternary systems is incomplete and characterised by specific drawbacks exemplified by manufacturing of the alloys only using a particular method, use of very high alloying elements additions to produce β Ti alloys, and lack of quantification of the structural behaviour, especially in terms of tensile properties. It is also worth mentioning that, to the best knowledge of the authors, no studies analysed the development of Ti-based quaternary alloys considering the simultaneous addition of these alloying elements (i.e. Al, Nb, Cu or Mn). Consequently, this study aims at quantifying the properties of quaternary Ti–Al–Nb–Cu and Ti–Al–Nb–Mn and clarify their work hardening behaviour. For that, the specific composition of the alloys was designed using current theories and produced via the blended elemental approach as it permits to easily change the chemistry of the alloy. Evaluation of physical properties, microstructural analysis, and mechanical characterisation were performed to be able to correlate the former with the latter based on the effects brought about by the changes in alloy chemistry.

2. Experimental procedure

In this study quaternary Ti alloys based on the concurrent addition of a α stabiliser and two β stabilisers were developed. In particular, Al was chosen as the α stabiliser and Nb simultaneously added with Cu or Mn were selected for β stabilisers. It is worth noticing that Nb is an isomorphous β stabiliser whereas both Cu and Mn are eutectoid β stabilisers. The raw materials acquired for the study, whose features are reported in Table 1, are commercial powders. These include a comminuted Ti powder, an atomised Al powder, a comminuted Nb powder, an electrolytic Cu powder, and a crushed Mn powder. As a consequence of their manufacturing methods the powders have different morphology and maximum particle size. It is worth mentioning that the starting Ti powder has an oxygen content of 0.27 wt%.

Table 1
Suppliers' specification details of the commercial raw materials used in the study.

Powder	Max particle size	Morphology	Purity	Supplier
Ti	<75 μm	Irregular	>99.4%	Goodfellow
Al	<45 μm	Spherical	>99.7%	Ecka Granules
Nb	<45 μm	Irregular	>99.8%	AlfAesar
Cu	<63 μm	Dendritic	>99.7%	Merck KGaA
Mn	<45 μm	Angular	>99.0%	Sigma-Aldrich

Powder blends of the desired compositions (i.e. Ti-2.5Al-xNb-xCu and Ti-2.5Al-xNb-xMn where x = 2 and 6 wt%) were obtained by means of mixing the raw materials at 45 rpm for 30 min in a V-shaped blender. Cylindrical samples (40 mm diameter and 20 mm thickness) were prepared via cold uniaxial pressing (600 MPa) followed by vacuum sintering (1300°C, 2 h, 10°C/min heating and cooling rate). These manufacturing conditions were chosen based on existing literature [45,46].

The response of the quaternary Ti alloys to the sintering process was quantified by analysing the variations of density, porosity, and densification parameter. The density of the as-pressed samples (i.e. green) was measured through the mass-to-volume ratio. The density of the sintered samples was obtained via water displacement measurements (ASTM B962). Relative density values were computed using the theoretical density of the quaternary Ti alloys as calculated via the rule of mixtures. Characterisation of the microstructure was performed using an Olympus BX-60-F5 optical microscope and a Hitachi S-4700 SEM/EDS elemental analysis. The classical metallographic route entailing SiC papers grinding and polishing was initially used, and the microstructural features were revealed by means of an aqueous Kroll reactant comprising 2 ml of HF and 4 ml of HNO_3. Confirmation of the phases present was done by means of XRD analysis (Philips X'pert, CuK_α radiation) scanning the samples at a rate of 0.013° with a dwell time of 0.5 s. The mechanical behaviour of the quaternary Ti alloys was quantified using dog-bone tensile specimens with 2 mm × 2 mm cross-section and at least three specimens per composition were tested. An Instron 33-R-4204 universal testing machine was used to pull the specimens a strain rate of $5{\cdot}10^{-3}$ s^{-1} while recording the elongation by means of a mechanical extensometer. The values of the yield strength of the quaternary Ti alloys was calculated by means the offset method (ASTM E8). Work hardening was defined as the ratio of the derivatives of the true stress divided by true plastic strain (i.e. $d\sigma/d\varepsilon_p$) calculated from the tensile data. Five individual measurements were performed to quantify the average Rockwell hardness (HRA) of the quaternary Ti alloys.

3. Results

The design of the quaternary Ti alloys entailing a α stabiliser and two β stabilisers was done through a combination of different theories and practical knowledge. Specifically, the molecular orbital method proposed by Morinaga [47], which considers the bond order and the *d*-electrons orbital energy, and the molybdenum equivalent (MoE) parameter were used. For the latter, both the definition proposed by Bania [48] (MoE = 0.28·Nb 0.77·Cu + 1.54·Mn – 1.00·Al) and by Wang et al. [49] (MoE = 0.28·Nb 1.50·Cu + 2.26·Mn – 1.47·Al) were considered. For practical reasons, the Al content was fixed and limited to 2.5 wt% and the ratio between the isomorphous (viz. Nb) and eutectoid (viz. Cu or Mn) kept constant. Two compositional variations (viz. 2 wt% and 6 wt%) were, therefore, chosen. The resulting quaternary alloys from this combined design approach were, thus, Ti-2.5Al–2Nb–2Cu, Ti-2.5Al–6Nb–6Cu, Ti-2.5Al–2Nb–2Mn, and Ti-2.5Al–6Nb–6Mn (Fig. 1). The bond order/*d*-electrons orbital energy map indicates that all

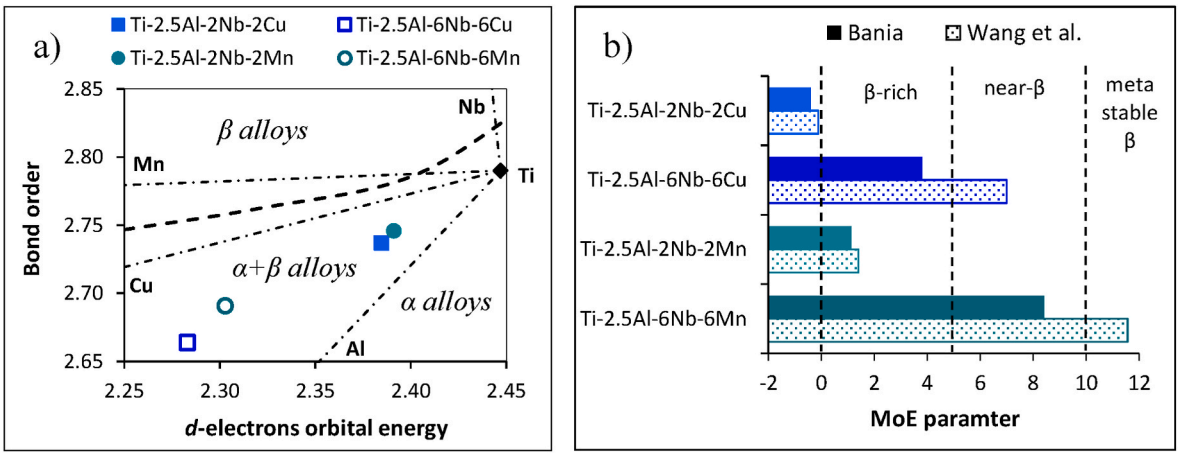

Fig. 1. Details of the theories used to design the quaternary Ti alloys: a) bond order/*d*-electrons orbital energy map, and b) molybdenum equivalent (MoE) parameter.

the quaternary Ti alloys are α+β Ti alloys (Fig. 1a). Conversely, a significant variability in terms of Ti alloy type is obtained when considering the MoE parameter depending on the type of alloying elements as well as depending on the actual chemistry of the quaternary alloy.

Fig. 2 shows the variation of the physical properties of the quaternary Ti alloys, including relative density, porosity, and densification parameter. It can be seen that the relative green density decreases (83.9 → 80.2%) with the amount of alloying elements and so does the relative sintered density (92.7 → 89.9%) whereas the gain in relative density increases (8.6 → 9.7%). Consequently, the amount of porosity left by the sintering process increases (7.3 → 10.1%) and the values of the densification parameter decrease (55.0 → 46.7%). It can be noticed that the Mn-bearing quaternary Ti alloys are generally characterised by higher relative density values and lower amount of residual porosity. However, there is a crossover in terms of densification parameter values.

Representative results of the microstructural characterisation performed on the quaternary Ti alloys, including low magnification optical micrographs, high magnification SEM micrographs, and elemental maps, are shown in Figs. 3–6. Fig. 3 shows that the Ti-2.5Al–2Nb–2Cu alloy is characterised by a lamellar microstructure composed of α grain boundaries and α+β lamellae. The morphology of the residual porosity is mainly spherical, although some elongated pores are also present (Fig. 3a). The α lamellae are quite coarse and, thus, the β lamellae are fine (Fig. 3b). A homogeneous distribution of the alloying elements was achieved due to the successful dissolution of the alloying elements powders with both Al and Nb evenly distributed within the two phases and Cu primarily found in the β phase (Fig. 3c–f).

The primary difference found between the Ti-2.5Al–2Nb–2Cu and Ti-2.5Al–6Nb–6Cu alloys is the coarseness of the microstructural features as the latter is still characterised by a lamellar microstructure but its features are much finer. Regularly distributed spherical pores are found within the microstructure but the number of irregular pores is higher (Fig. 4a) due to the lower relative density (Fig. 2a). The width of the α lamellae is smaller and that of the β larger as a consequence of the stabilisation of a higher amount of β phase (Fig. 4b). Complete dissolution of the powder particles was achieved resulting in a homogeneous distribution of the alloying elements (Fig. 4c–f) with Cu still segregated in the β phase.

Fig. 5 shows the results of the microstructural analysis of the Ti-2.5Al–2Nb–2Mn alloy where it can be seen that the alloy is characterised by a lamellar microstructure and primarily elongated residual porosity (Fig. 5a). The overall appearance of the microstructure is not remarkably different from that of the Ti-2.5Al–2Nb–2Cu alloy (Fig. 3) but the microstructural features are finer as Mn is a stronger β stabilisers compared to Cu (Fig. 1). The distribution of the alloying elements is homogeneous and partitioning of Mn in the β phase is clearly visible from the elemental maps (Fig. 5c–f).

In the case of the Ti-2.5Al–6Nb–6Mn alloy, the alloy still has a lamellar microstructure and elongated residual pores and the size of the lamellae is significantly smaller (Fig. 6a) in comparison to both the Ti-2.5Al–2Nb–2Mn and the Ti-2.5Al–6Nb–6Cu alloys. The chemistry of the alloy is fully homogeneous, indicating the complete dissolution of the

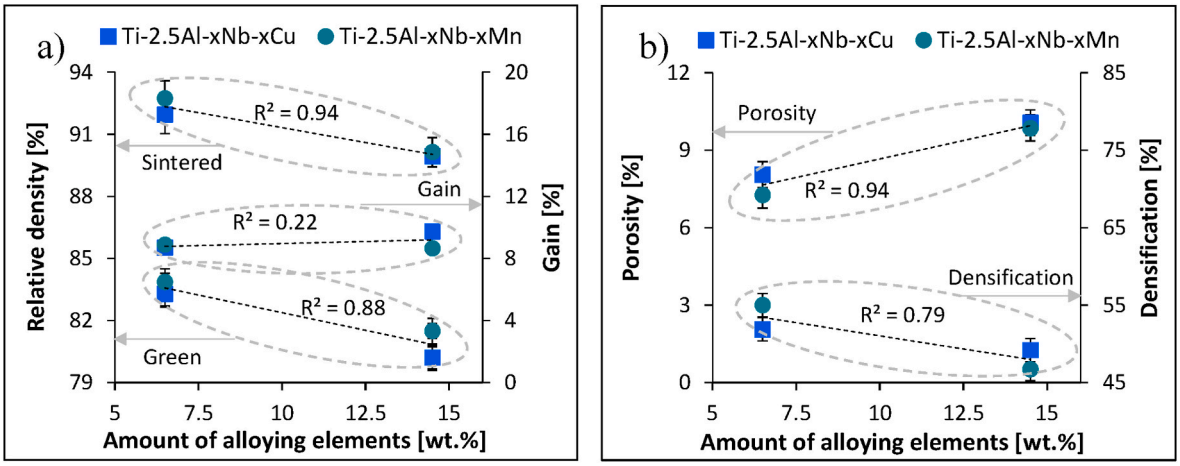

Fig. 2. Variation of the physical properties of the quaternary Ti alloys: a) relative density and associated gain, and b) porosity and densification.

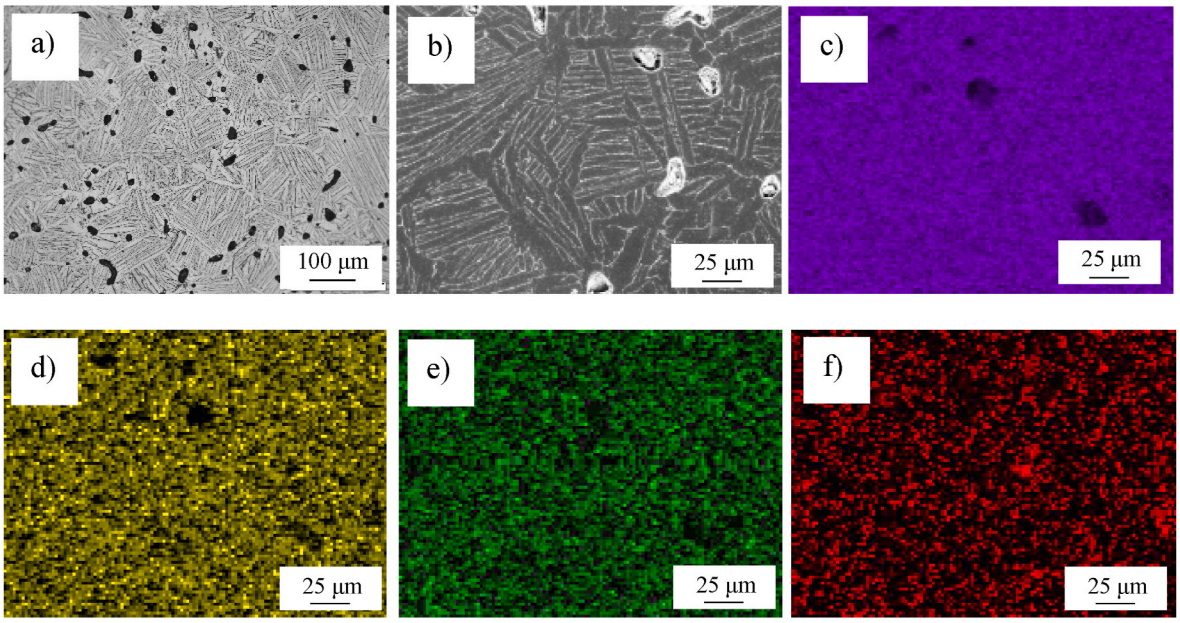

Fig. 3. Representative results of the microstructural characterisation of the Ti-2.5Al–2Nb–2Cu alloy: a), optical micrograph, b) SEM micrograph, c) Ti map, d) Al map, e) Nb map and, f) Cu map.

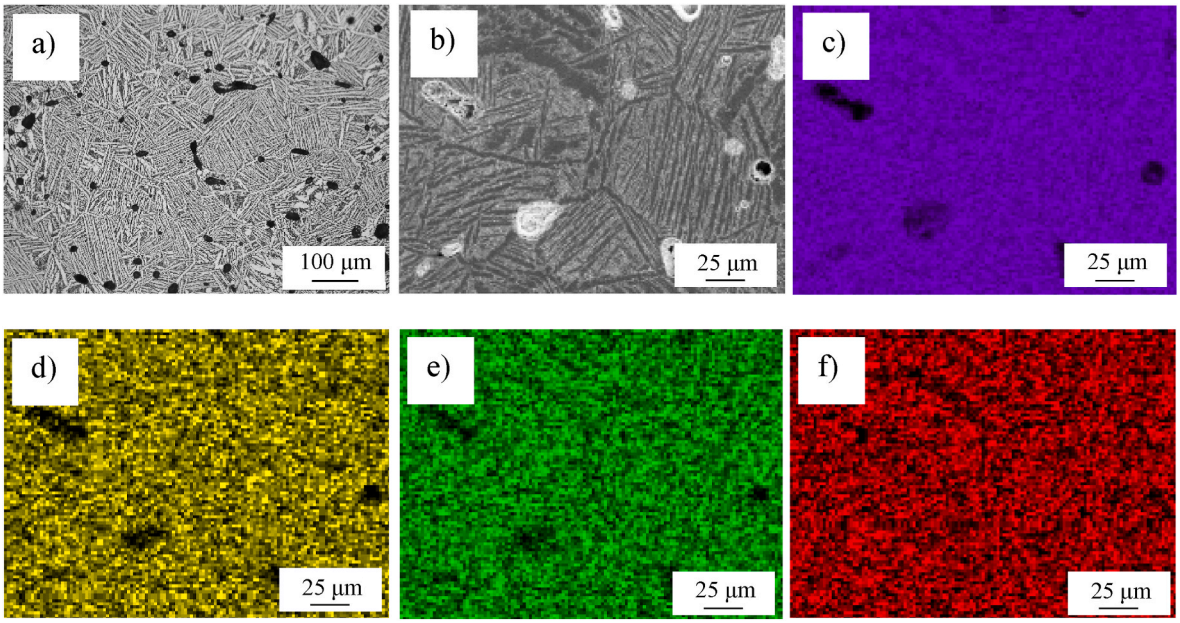

Fig. 4. Representative results of the microstructural characterisation of the Ti-2.5Al–6Nb–6Cu alloy: a), optical micrograph, b) SEM micrograph, c) Ti map, d) Al map, e) Nb map and, f) Cu map.

alloying elements powder particles (Fig. 6c–f), and enrichment in Mn of the β phase is still happening although less discernible in the elemental map due to the smaller size of the α+β lamellae.

From the XRD patterns of the quaternary Ti alloys shown in Fig. 7 it is found that the equilibrium α phase is always the predominant, regardless of the chemistry of the alloy. The primary peak of the equilibrium β phase was detected in all the alloys, with the exception of the Ti-2.5Al–2Nb–2Cu alloy. For the latter the amount of β phase is below the detection limit of the equipment. The relative intensity of the main β phase's peak increases with the amount of alloying elements and it is stronger in the case of the Mn-bearing quaternary Ti alloys. It is worth noticing that the primary peak of the Ti_2Cu intermetallic phase was also detected in the case of the Cu-bearing quaternary Ti alloys where its relative intensity slightly increases with the amount of Cu added. No other metastable phases or Mn-based intermetallics were detected.

Fig. 8 shows the results of the mechanical characterisation performed on the quaternary Ti alloys. From the representative stress-strain tensile curves, it can be seen that the quaternary Ti alloys are characterised by an elastic + plastic deformation behaviour regardless of their actual chemical composition. The tensile curves of the quaternary Ti alloys overlap in the elastic region, indicating a similar elastic stiffness. Both the yield stress (YS) and the ultimate tensile strength (UTS) increase with the amount of alloying elements and higher values are achieved in the Mn-bearing quaternary Ti alloys (Fig. 8b). Specifically, YS increases from 644 MPa to 714 MPa and from 658 MPa to 869 MPa, respectively, for the Cu- and Mn-bearing quaternary Ti alloys. Similarly,

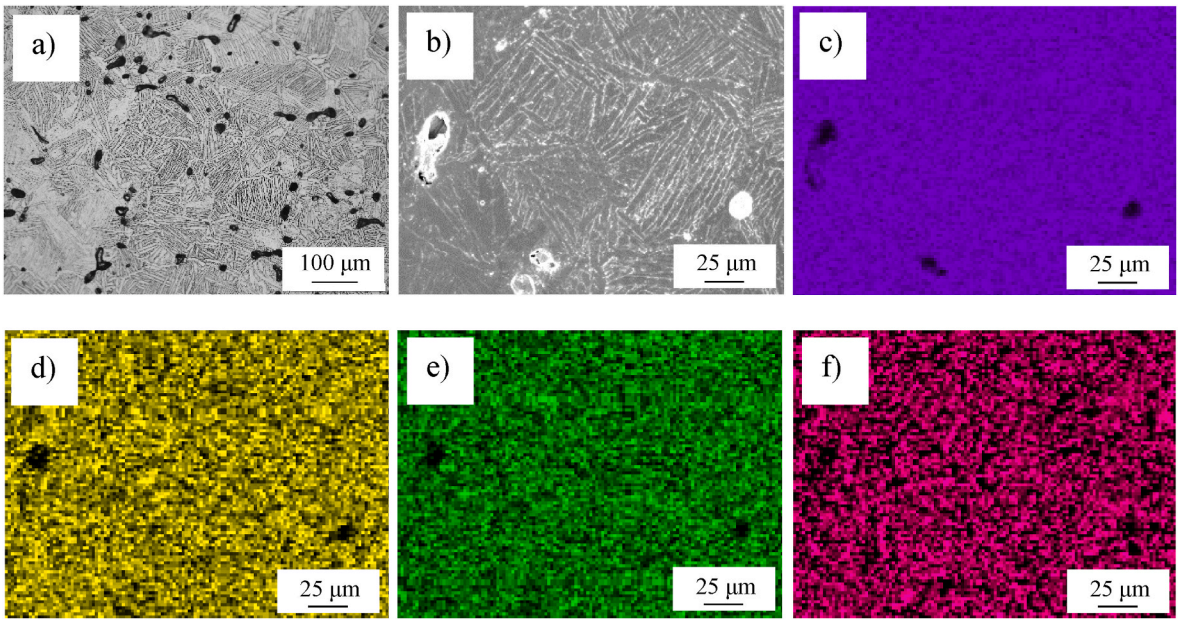

Fig. 5. Representative results of the microstructural characterisation of the Ti-2.5Al–2Nb–2Mn alloy: a), optical micrograph, b) SEM micrograph, c) Ti map, d) Al map, e) Nb map and, f) Mn map.

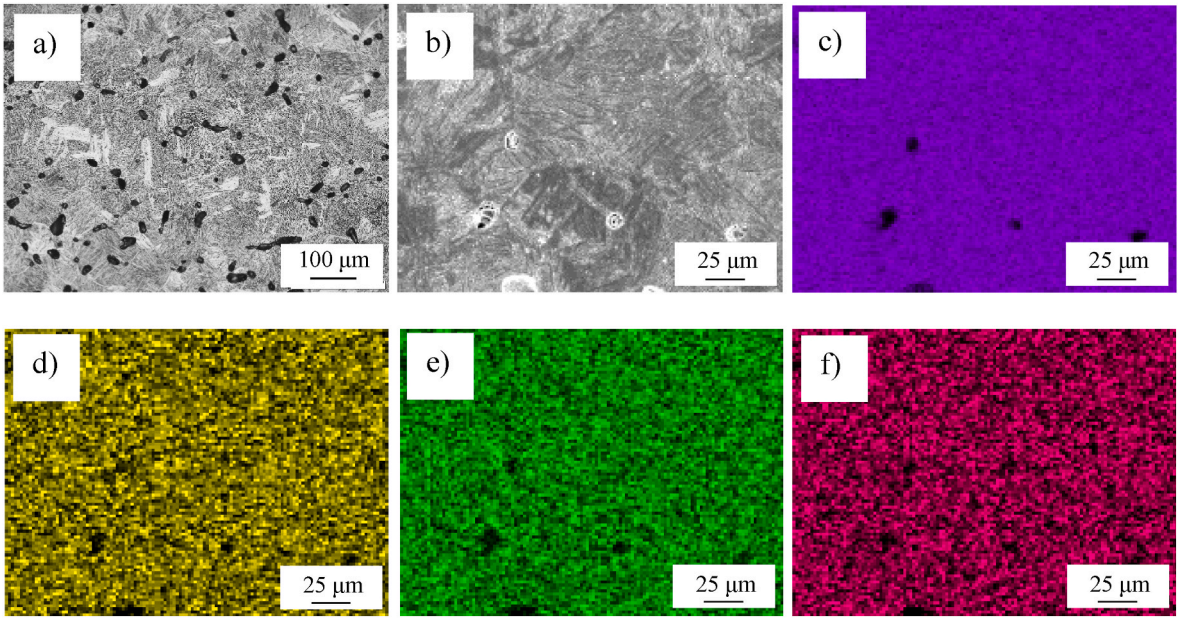

Fig. 6. Representative results of the microstructural characterisation of the Ti-2.5Al–6Nb–6Mn alloy: a), optical micrograph, b) SEM micrograph, c) Ti map, d) Al map, e) Nb map and, f) Mn map.

UTS increases from 718 MPa to 784 MPa and from 732 MPa to 914 MPa, respectively, for the Cu- and Mn-bearing quaternary Ti alloys. Concurrently, the elongation at fracture, respectively, decreases from 6.0% to 3.5% and from 5.0% to 2.8% (Fig. 8c). A linear increase of the average hardness (Fig. 8d) is also found with the Mn-bearing quaternary Ti alloys (59.5 → 62.3 HRA) being harder than their Cu-bearing counterparts (58.2 → 60.2 HRA). It is worth mentioning that error bars correspond to the standard deviation of at least three tested samples. If not visible, the error bar is $< \pm 10$ MPa for the strength, $\pm 0.1\%$ for the elongation, and ± 0.2 HRA for the hardness, respectively.

The results of the fractographic analysis performed on the fracture surface of the tensile samples of the quaternary Ti alloys are displayed in Fig. 9. It can be seen that the facture surface of the Ti-2.5Al–2Nb–2Cu alloy is the typical of ductile metals and, thus, composed of dimples primarily derived from the plastic deformation of the residual pores. The alloy failed due to the intergranular fracture of the α grain boundaries, therefore generating shallow tear ridges, as well as fracture along the interlamellar boundaries (Fig. 9a and b). In the case of the Ti-2.5Al–6Nb–6Cu alloy, similar features are found but few areas fractured transgranularly are also present and the amount of dimples is lower (Fig. 9c and d). The fracture surface of the Mn-bearing quaternary Ti alloys presents a significantly higher amount of smooth areas fractured transgranularly, a lower number of ductile dimples, and deeper tear ridges (Fig. 9e and f). Less plastically deformed residual pores and a higher number of brittle areas are found as the amount of alloying elements increases (Fig. 9g and h).

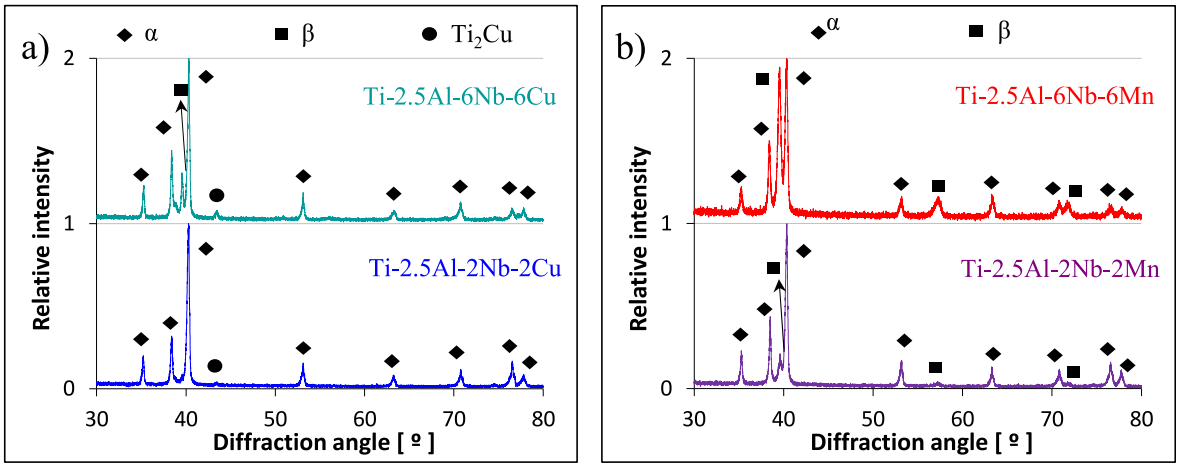

Fig. 7. XRD patterns of the quaternary Ti alloys: a) Ti-2.5Al-xNb-xCu, and b) Ti-2.5Al-xNb-xMn.

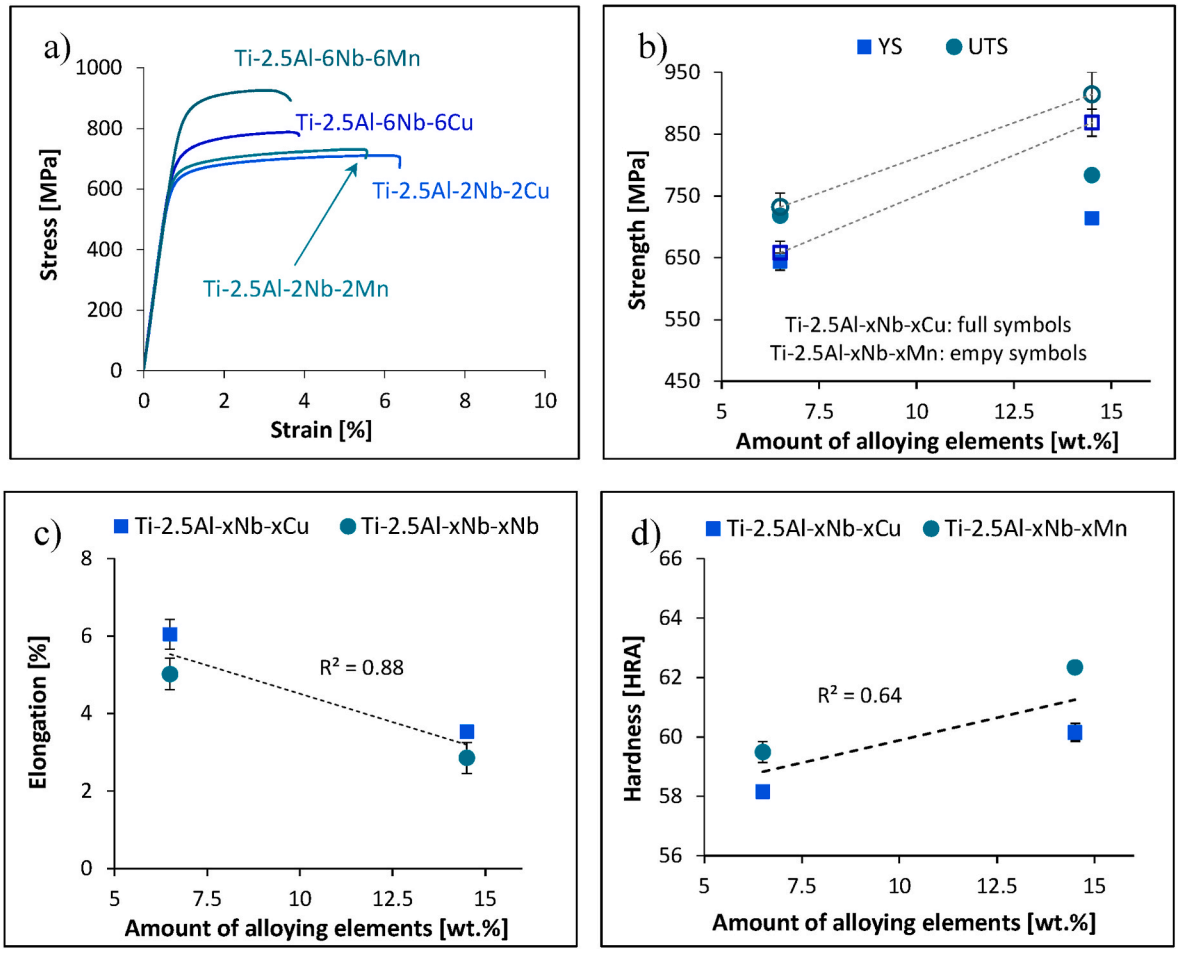

Fig. 8. Mean mechanical properties of the quaternary Ti alloys: a) representative stress-strain tensile curves, yield stress (YS) and ultimate tensile strength (UTS), c) elongation at fracture, and d) hardness.

4. Discussion

This study considered the design, manufacturing, and characterisation of new quaternary Ti alloys entailing the simultaneous addition of a α stabiliser (viz. Al), an isomorphous β stabiliser (viz. Nb), and a eutectoid β stabiliser (viz. Cu or Mn). The quaternary alloys are to be manufactured via the conventional powder metallurgy route of press and sinter and, therefore, commercial powders were purchased and they are characterised by different morphologies and maximum particle sizes (Table 1). The quaternary alloys were designed on the basis of the molecular orbital method [47] and the MoE parameter [48,49] resulting in the Ti-2.5Al–2Nb–2Cu, Ti-2.5Al–6Nb–6Cu, Ti-2.5Al–2Nb–2Mn, and Ti-2.5Al–6Nb–6Mn chemical compositions (Fig. 1). The bond order/-*d*-electrons orbital energy map shows that the quaternary Ti alloys all rest within the α+β two-phase field but they are obviously spread as a consequence of the intrinsic effect of each one of the alloying elements

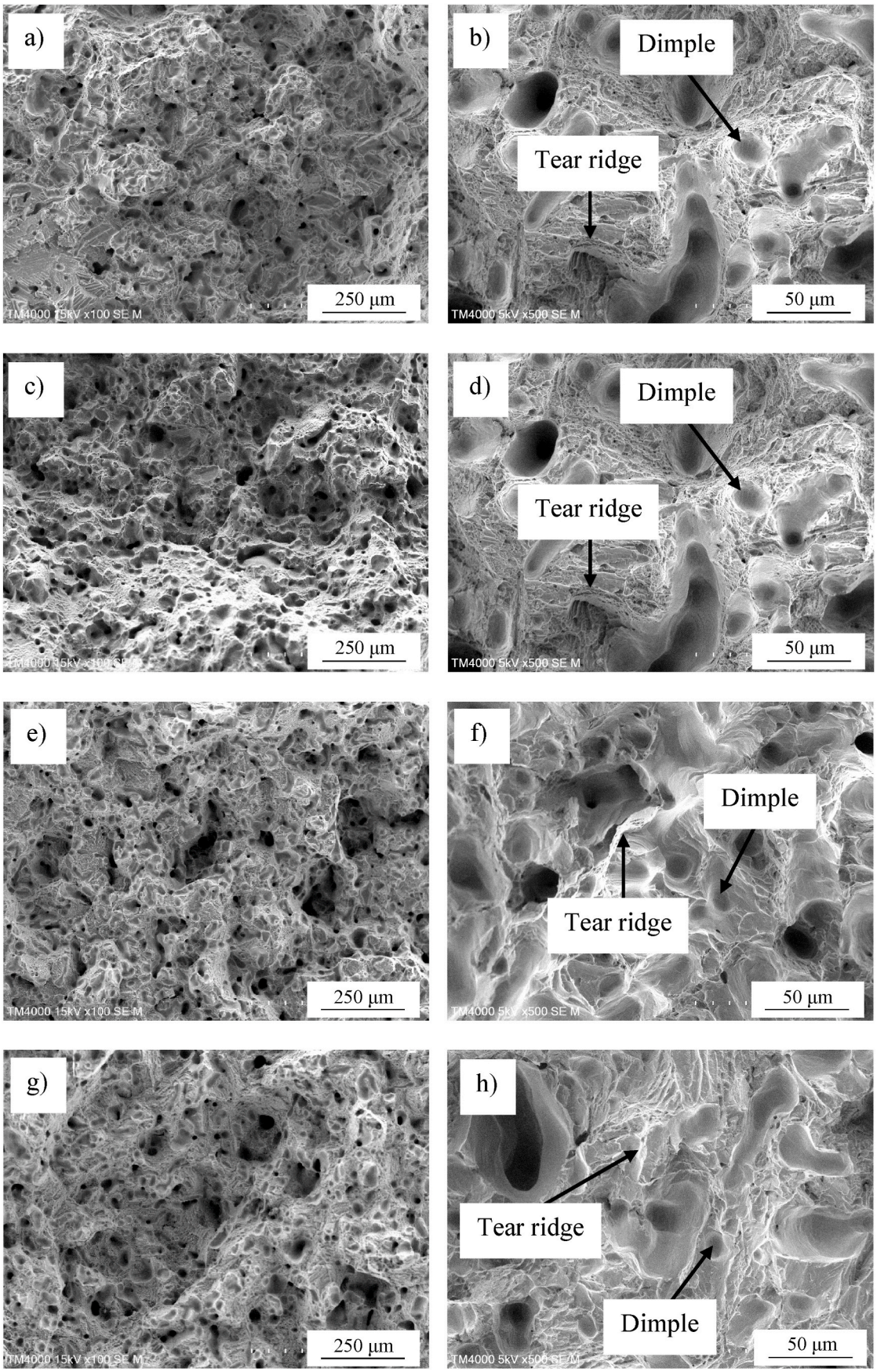

Fig. 9. Representative results of the fractographic analysis of the metastable Ti alloys (low and high magnification, respectively): a-b) Ti-2.5Al–2Nb–2Cu, c-d) Ti-2.5Al–6Nb–6Cu, e-f) Ti-2.5Al–2Nb–2Mn, and g-h) Ti-2.5Al–6Nb–6Mn.

(Fig. 1a). However, it can be noticed that the addition of Cu leads to alloys characterised by lower bond order/*d*-electrons orbital energy' pairs values. This is due to the fact that Cu is a weaker β stabiliser with respect to Mn (Fig. 1). This is confirmed by the MoE parameter values (Fig. 1b) as the Cu-bearing quaternary Ti alloys have lower values compared to the respective Mn-bearing alloys. For each quaternary system, a higher MoE is obtained for higher additions of Cu or Mn. The classification of Ti alloys proposed by Cotton et al. [50] was used. It can be seen that the discrepancy between the two definitions of the MoE parameter increases as does the amount of alloying elements. Consequently, it is found that Ti-2.5Al–2Nb–2Cu is a α+β Ti alloy and Ti-2.5Al–2Nb–2Mn is a β-rich α+β Ti alloy. Ti-2.5Al–6Nb–6Cu is either a β-rich α+β or a near-β Ti alloy depending on the definition of the MoE parameter used. Similarly, Ti-2.5Al–6Nb–6Mn is classified either as near-β or metastable β Ti alloy. The inconsistency between the molecular orbital method [47] and the MoE parameter [48,49] lies on the fact that the former is based on equilibrium conditions while the latter is generally not. It is worth noticing that the relative green density and sintered density values achieved in the quaternary Ti alloys are comparable to those of Ti [51] other Ti alloys [3,4,52] obtained by means of the blended elemental approach as the main vacuum sintering parameters used (i.e. 1300°C and 2 h) are amongst the most commonly used to sinter Ti alloys [45,46]. If higher relative density values are needed, a pressure-assisted methods like Spark Plasma Sintering could be used as demonstrated by Zhang et al. using Ti–Mn alloys [53].

From the analysis of the variation of the physical properties of the quaternary Ti alloys (Fig. 2), it is found that the addition of a greater amount of alloying elements reduces the relative green density. This means that the compressibility of the powder blends of the quaternary Ti alloys decreases due to the mismatch in terms of morphology, particle size, and relative hardness. Specifically, the spherical and dendritic morphology of the Al and Cu powders is more detrimental than the irregular and angular morphology of the Nb and Mn powders. Therefore, the Cu-bearing quaternary Ti alloys generally have lower relative green density values and the gap between the two types of alloys increases with the amount of alloying elements. It is also found that the relative sintered density Cu-bearing quaternary Ti alloys is lower with respect to their Mn-bearing equivalents (Fig. 2a). Nevertheless, it can be seen that the gap between the two decreases as the amount of alloying elements increases, which is reflected in a decreasing gap between the amount of residual porosity (Fig. 2b). Accordingly, the relative density gain becomes more pronounced for the Cu-bearing quaternary Ti alloys. As the difference between the two types of alloys is the content of the eutectoid β stabiliser, it is inferred that the addition of Cu leads to a better sinterability compared to Mn. This is confirmed from the crossover of the values of the densification parameter, which is higher for the Cu-bearing quaternary Ti alloys at higher additions of alloying elements. This behaviour is primarily connected to the intrinsic diffusivity of the alloying elements in Ti where Cu dissolves faster than Mn, despite its slightly bigger particle size (Table 1), due to its lower melting point.

From the results of the microstructural characterisation performed on the quaternary Ti alloys (Figs. 3–6) it is found that all the alloys have residual porosity present in the microstructure where the volumetric percentage agrees with the data of Fig. 2. A combination of spherical and elongated pores is present where the relative amount of elongated pores increases with the amount of alloying elements and their percentage is greater in the Mn-bearing quaternary Ti alloys with respect to the Cu-bearing alloys. Regardless of their actual chemistry, the quaternary Ti alloys are all characterised by a lamellar microstructure composed of α grain boundaries (i.e. prior β grains) and α+β lamellae. This microstructure is typical of Ti alloys entailing α and β stabilisers in their chemical composition and commonly forms upon the slow cooling of the alloy when crossing its allotropic phase transformation temperature (viz. β transus). Generally, a refinement of the microstructural features including the size of the prior β grains as well as that of the α+β lamellae is achieved for higher alloying elements addition rates. Moreover, the fineness of the lamellar microstructure is significantly superior in the Mn-bearing quaternary Ti alloys as a consequence of the greater amount of stabilised β phase within the microstructure. This is due to the fact that Mn is a stronger β stabilisers compared to Cu (Fig. 1). This is corroborated by the results of the XRD analysis (Fig. 7) where it is found that the α phase is always the predominant but the relative intensity of the β phase' primary peak increases with the amount of Cu and Mn added and it is stronger in the case of the Mn-bearing quaternary Ti alloys. Both elemental mapping and XRD confirm that the selected sintering conditions (i.e. 1300°C during 2 h) are sufficient to completely dissolve the alloying elements powder particles. Therefore, a homogeneous distribution of the alloying elements is achieved regardless of the chemical composition. However, partitioning of the eutectoid β stabilisers occurs as expected from the respective binary phase diagrams [54]. Moreover, it is found that the presence of Cu in the quaternary Ti alloys leads to the precipitation of the Ti_2Cu intermetallic phase through the eutectoid reaction, but no other metastable phases or Mn-based intermetallics were detected. Formation of the brittle Ti_2Cu intermetallic phase in binary Ti–Cu alloys has been previously reported in literature for different amount of Cu depending on the manufacturing technique used [21–26].

The characterisation of the tensile behaviour of the quaternary Ti alloys shows that, independently of their chemistry, the alloys undergo both elastic and plastic deformation upon uniaxial loading. The transition from one behaviour to the next is shifted towards higher loads as the amount of alloying elements increases and, consequently, the amount of plastic deformation withstood decreases (Fig. 8a). For each alloy system, a linear increase of both YS and UTS is, thus, found but the increment rate is significantly different as the Mn-bearing quaternary Ti alloys are stronger that their Cu-bearing counterparts. In particular, an average increase in strength of 68 MPa is obtained when the amount of Cu and Nb is increased from 2% to 6% whereas an average increase of 196 MPa is attained for the progressive addition of Mn and Nb (Fig. 8b). As the alloys become stronger, their ability to plastically deform decreases where the average ductility loss between the Cu- and Mn-bearing quaternary Ti alloys is comparable, i.e. 2.5% vs. 2.2% (Fig. 8c). The embrittlement of the quaternary Ti alloys for higher addition of alloying elements is echoed by the relative decrease of the amount of ductile dimples and by the increase of faceted fractured areas in their fracture surface (Fig. 9). The effect of the specific β eutectoid stabiliser is reflected on the switch of the fracture surface from rough to smooth as Mn is added instead of Cu. The change in tensile properties described is associated with the monotonic increment of the hardness with the Mn-bearing quaternary Ti alloys being harder and characterised by a slightly higher incremental rate with the addition of a greater amount of Mn and Nb (Fig. 8d).

The overall mechanical behaviour found for the quaternary Ti alloys is primarily linked to the effects brought about by the type of alloying elements used and their addition rates. The quaternary Ti alloys become stronger for higher alloying elements addition rates due to solid solution strengthening, which is directly related to the total amount of alloying elements. However, each element has a different β stabilisation power, with Mn being significantly more effective in stabilising the β phase with respect to Cu (Fig. 1). This obviously reflects on the stabilisation of a greater amount of β phase within the microstructure, which is stronger than the α phase, but also on the associated refinement of the microstructural features. Finer interlamellar spacing are known to be more effective in hindering the movement of dislocations in α+β Ti alloys [55]. In the case of the Cu-bearing quaternary Ti alloys, eutectoid precipitation of the hard and brittle Ti_2Cu intermetallic phase also occurs, which contributes to the strengthening of the alloys. However, this still does not result in the Cu-bearing quaternary Ti alloys being stronger that their Mn-bearing equivalents. Finally, in this instance, the addition of the different alloying elements also affect the compressibility and amount of residual porosity left by the sintering process. From the graphs of the variation of the mean mechanical properties of the

quaternary Ti alloys as a function of porosity, it can be seen that both strength (Fig. 10a) and hardness (Fig. 10c) increase whereas the elongation at fracture decreases (Fig. 10b) as the total amount of porosity increases. This highlights that the presence of the residual pores detracts from the theoretical strength and hardness of fully dense quaternary Ti alloys but it is not the primary aspect controlling these properties. In the case of the ductility, the residual porosity synergistically work alongside the different acting strengthening mechanisms to decrease the ability of the quaternary Ti alloys to plastically deform. However, the fact that the Cu-bearing quaternary Ti alloys have higher elongation at fracture values in comparison to the Mn-bearing alloys, despite their higher amount of porosity (Fig. 2) and the presence of the Ti_2Cu intermetallic phase (Fig. 7), indicates that these two factors are not the ones primarily controlling the ductility of the quaternary Ti alloys. The mechanical behaviour and properties presented are also influenced by the oxygen content, which in this case is higher than the typical maximum content specified for α+β Ti alloys (i.e. 0.20 wt%), due to the oxygen content of the starting Ti powder.

The typical work hardening behaviour of the late stage of deformation of the quaternary Ti alloys is shown in Fig. 11 where it can be seen that the overall work hardening curve is similar amongst the alloys, reflecting a similar deformation mechanism. This is due to the fact that all the quaternary Ti alloys have a lamellar microstructure (Figs. 3–6) regardless of their actual chemistry. The asymptotic part of the curve, which is not a real deformation stage for polycrystalline materials [56], is known as Stage II and is characterised by high work hardening values and a sharp work hardening decrements over small true plastic strain increments. At approximately 0.015 true plastic strain, the quaternary Ti alloys switch to Stage III, which is governed by the compromise between the generation and annihilation of dislocations. In Stage III the work hardening rate decreases more gently and stabilises at values around E/50 where the actual slope is alloy dependent. Shaper decrements are found for higher alloying elements addition rates and in the Mn-bearing quaternary Ti alloys compared to their Cu-bearing counterparts (Fig. 11a). From the detail of the asymptotic part of the work hardening curve (Fig. 11b), it can be seen that the position of the curve shift towards the right (viz. higher true plastic deformation values) for higher alloying elements addition rates and when Mn is used rather than Cu, which concludes in the decrease of the uniform ductility of the quaternary Ti alloys. This is related to the fineness of the lamellar microstructure, which is refined by both a higher amount of alloying elements and by the use of stronger β stabilisers. It can be noticed that the trend is reversed as the work hardening of the quaternary Ti alloys progresses in stage III due to the less restricted dislocations movement in the alloys with a coarser lamellar microstructure.

The necking stability Considère criterion states that necking of the material subjected to tensile loading begins at the intersection between the work hardening rate curve and the true stress-true strain tensile curve [57]. From Fig. 11c), it can be seen that there is strong correlation between the necking onset and Stage III of work hardening. In all the quaternary Ti alloys necking is followed by an increase in uniform elongation but its extent is related to the actual chemistry of the alloy. This correlates well with the ability to plastically deform of each quaternary Ti alloy (Fig. 8c) and it is related to their specific toughness. Therefore, necking onset happens in the Ti-2.5Al–6Nb–6Mn alloy and this leads to its failure soon after, which can be seen from the sudden

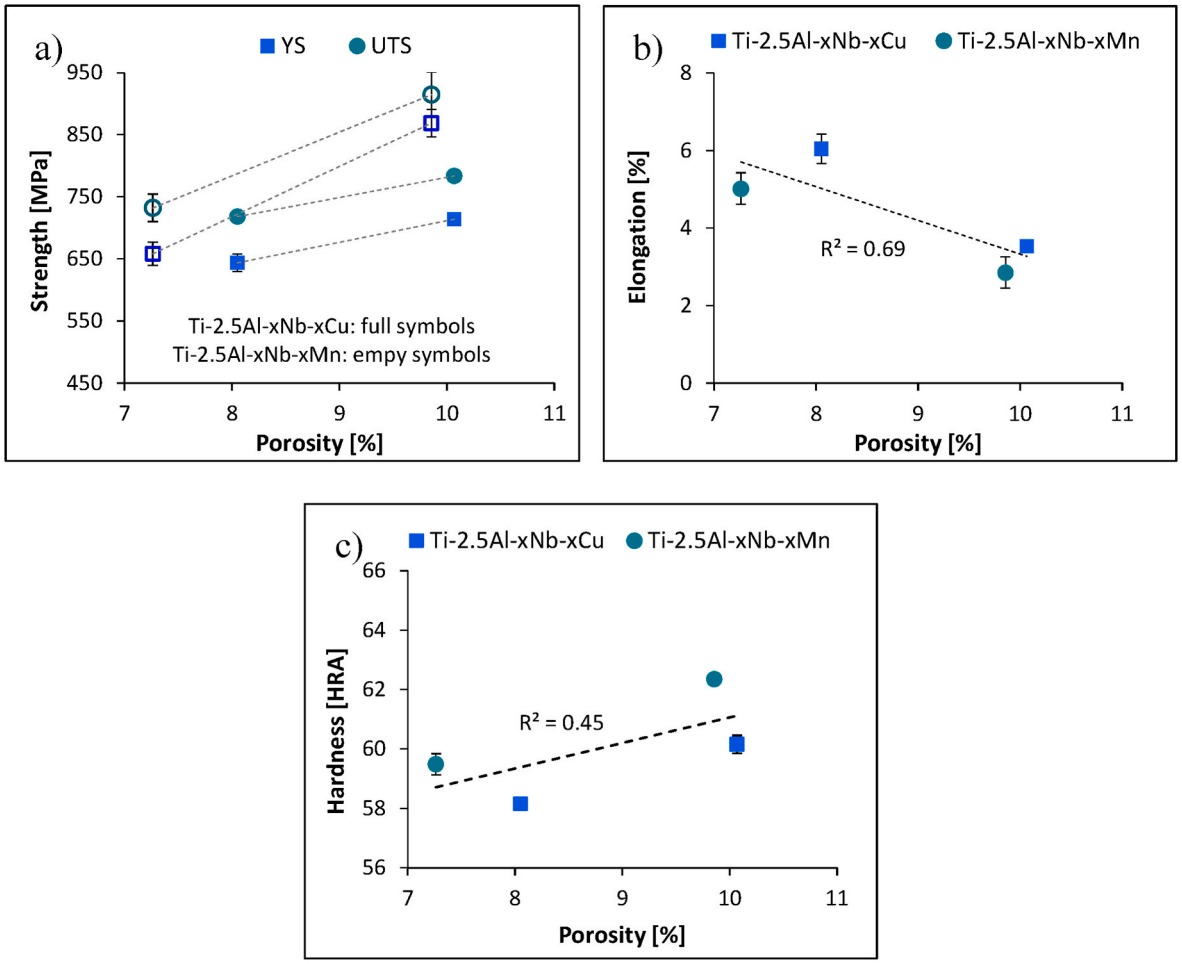

Fig. 10. Mean mechanical properties of the quaternary Ti alloys as a function of porosity: a) YS and UTS, b) elongation at fracture, and c) hardness.

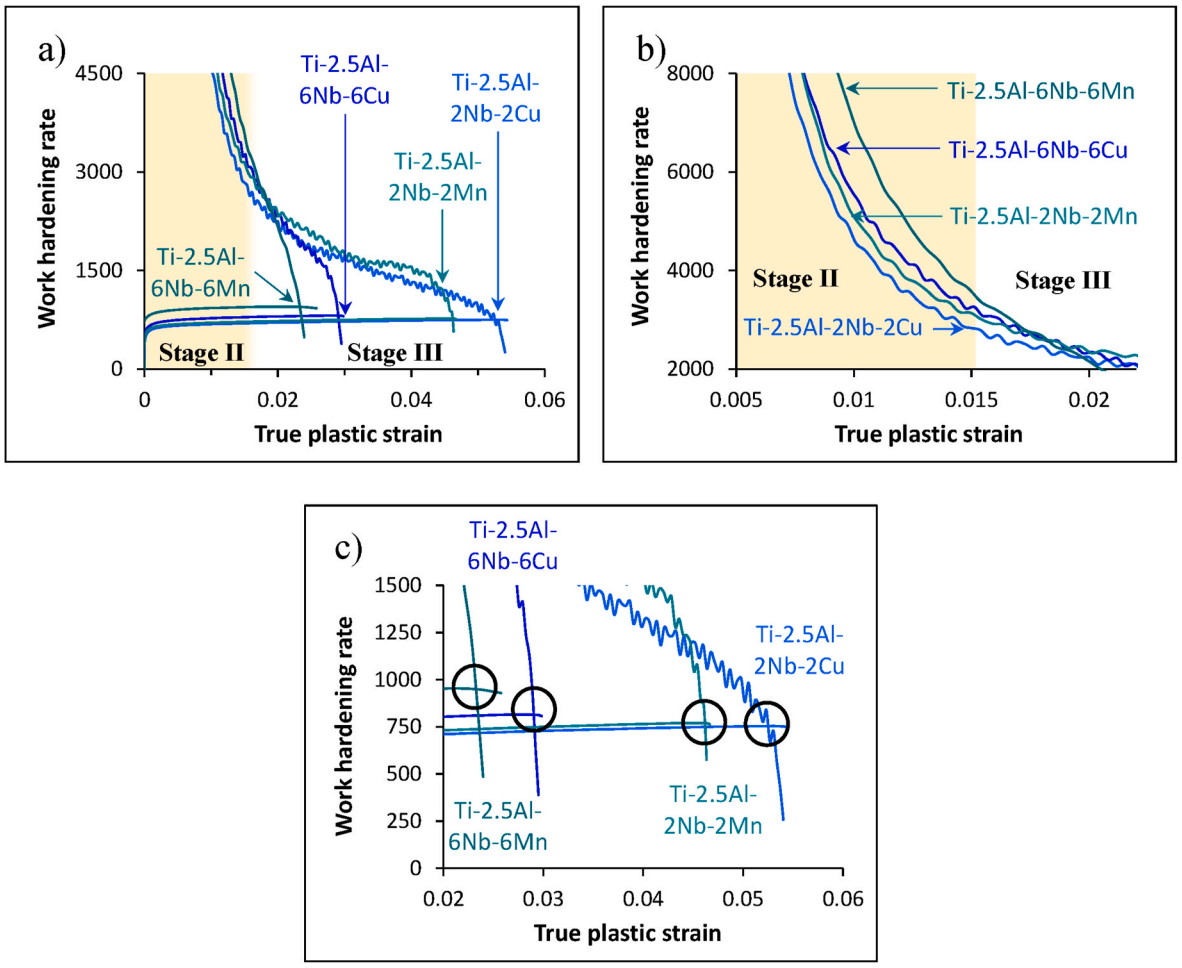

Fig. 11. Work hardening behaviour of the quaternary Ti alloys: a) overall work hardening rate versus true plastic strain, b) detail of the asymptotic part of the work hardening curve, and c) detail of the necking instability.

drop of the work hardening rate curve on crossing the true stress-true strain curve. Similar behaviour is found in the Ti-2.5Al–6Nb–6Cu alloy although necking is shifted towards a higher true plastic strain value as a consequence of the coarser lamellar microstructure. Conversely, the Ti-2.5Al–2Nb–2Cu and Ti-2.5Al–2Nb–2Mn alloys withstand a significantly higher amount of plastic deformation after necking as their work hardening rate curves decreases at a lower rate and the intersection of the curves occurs at much higher true plastic strain values.

Fig. 12 shows a comparison of the mechanical properties of the quaternary Ti-2.5Al-xNb-xCu alloys with alloys bearing similar alloying elements, manufactured via different methods, including sintered Ti-(10–22)Nb alloys [17], wrought Ti-(5–20)Nb alloys [58], cast Ti-(0.5–5) Cu alloys [21], sintered Ti-(2–10)Al-(1–5)Cu alloys [59,60], and cast Ti-(1–4)Cu-(6–24)Nb alloys [39]. From the variation of UTS versus hardness (Fig. 12a), it can be seen that the quaternary Ti-2.5Al-xNb-xCu alloys align with the general behaviour of higher UTS for higher hardness, which is related to the amount if alloying elements added. However, the quaternary Ti-2.5Al-xNb-xCu alloys have higher UTS for comparable hardness with respect to wrought Ti–Nb alloys, sintered Ti–Al–Cu alloys, and cast Ti–Cu alloys. The UTS is still comparable, even though the hardness is lower, with respect to cast Ti–Cu–Nb alloys. Concerning the variation of YS versus the amount of alloying elements (Fig. 12b), quaternary Ti-2.5Al-xNb-xCu alloys have higher YS in comparison to sintered and wrought Ti–Nb alloys as well as cast Ti–Cu–Nb alloys. A large amount of β stabilisers is generally needed to achieve a similar increment in YS with respect to when an α stabiliser is concurrently added with β stabilisers. In the case of the elongation at fracture versus the MoE parameter (Fig. 12c), the ductility of the quaternary Ti-2.5Al-xNb-xCu alloys is comparable to most alloys but lower with respect to sintered Ti–Al–Cu alloys and wrought Ti–Nb alloys. This is, respectively, related to the fineness of the microstructural features (i.e. balance between α and β stabilisers) and the presence of residual pores within the microstructure.

A comparison of the mechanical properties of the quaternary Ti-2.5Al-xNb-xMn alloys with alloys with comparable chemistry obtained using different processes including sintered Ti-(10–22)Nb alloys [17], wrought Ti-(5–20)Nb alloys [58], sintered Ti-(10–14)Mn alloys [28], sintered Ti-2.5Al-(1–10)Mn alloys [61], and welded Ti–2Al–2Mn alloys [62] is shown in Fig. 13. Analysing the variation of UTS versus hardness (Fig. 13a), it can be seen that the quaternary Ti-2.5Al-xNb-xMn alloys have higher UTS in comparison to all the other alloys, even when their hardness is lower with respect to those alloys. Once again, a general increasing trend between UTS and hardness is found as proportional to the amount of alloying elements. Regarding the YS, the quaternary Ti-2.5Al-xNb-xMn alloys are stronger than sintered and wrought Ti–Nb alloys, welded Ti–2Al–2Mn alloys, and most of the sintered Ti–Mn alloys. Porosity and manufacturing conditions have an impact on YS when alloys with the same composition are compared. The variation of the elongation at fracture versus the MoE parameter (Fig. 13c) shows that the behaviour of the quaternary Ti-2.5Al-xNb-xCu alloys aligns with that of other alloys, with the exception of the sintered Ti–Mn alloys where the latter are characterised by an equiaxed β microstructure. The ductility of the quaternary Ti-2.5Al-xNb-xCu alloys is lower compared to wrought Ti–Nb alloys and welded Ti–2Al–2Mn alloys due to the

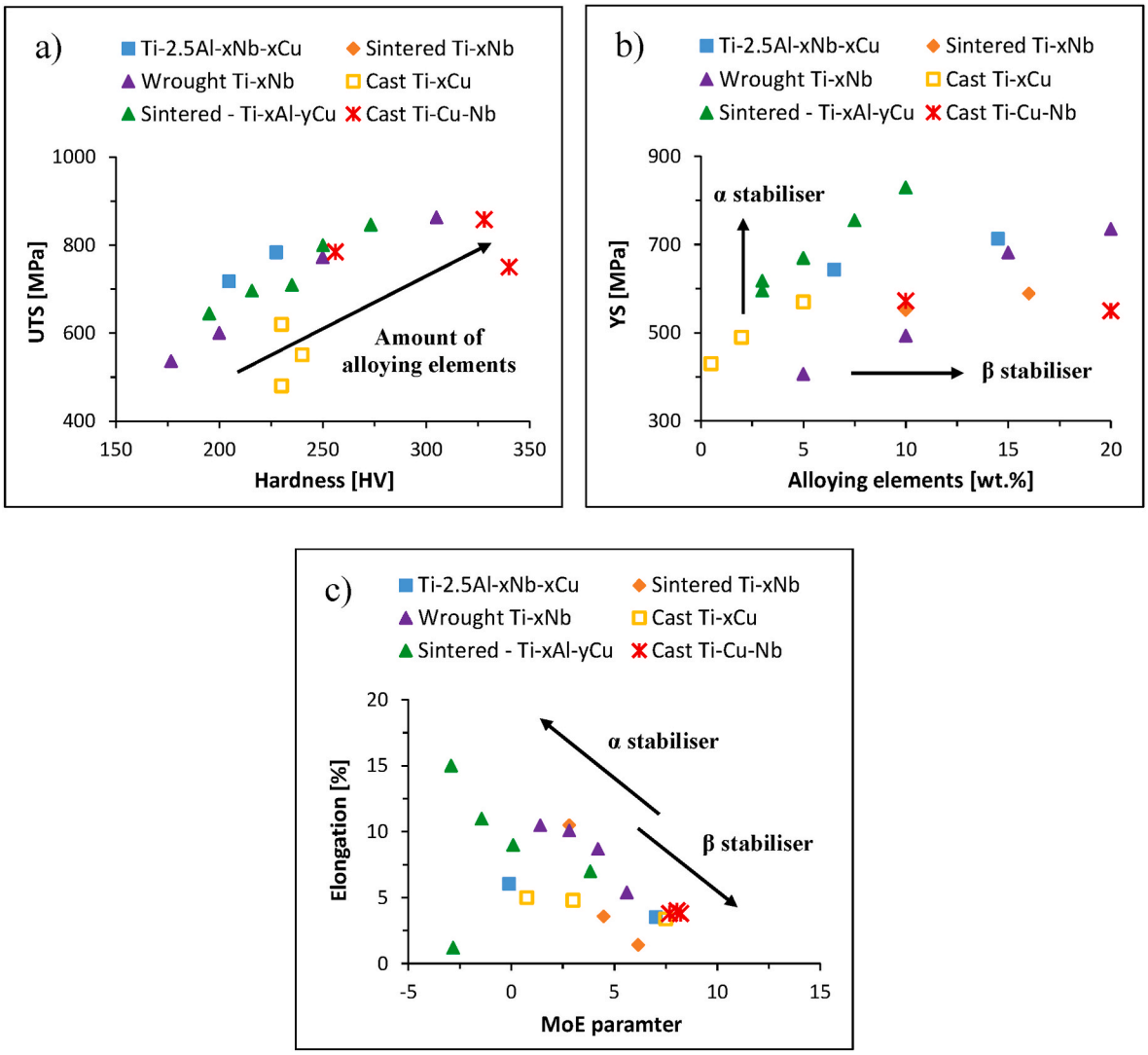

Fig. 12. Comparison of the mechanical properties of the quaternary Ti-2.5Al-xNb-xCu alloys with literature [17,21,39,58–60]: a) UTS versus hardness, b) YS versus total amount of alloying elements, and c) elongation at fracture versus MoE parameter.

presence of the residual porosity.

5. Conclusions

In this study quaternary Ti alloys involving the simultaneous addition of Al as α stabiliser and Nb and Cu or Mn as β stabilisers were designed on the basis of current theories (molecular orbital method and molybdenum equivalent parameter). These alloys were manufactured via cold uniaxial pressing followed by vacuum sintering to analyse their performance. The compressibility of the powder blend decreases as the amount of alloying elements increases due to the compromise between different powder morphologies, particle sizes, and intrinsic hardness of the elements. Sintering increases the relative density, does not reverse the decreasing trend of the density with the amount of alloying elements, but reduces the density gap between the Cu- and Mn-bearing quaternary Ti alloys due to the faster diffusion of Cu with respect to Mn. However, the Mn-bearing quaternary Ti alloys still have slightly lower amount of residual porosity compared to the Cu-bearing alloys. All the quaternary Ti alloys have residual pores and a lamellar microstructure where the shape of the pores switches from spherical to elongated when the alloying elements content is increased. The latter also leads to a progressive refinement of the microconstituents and finer microstructures are obtained when Mn rather than Cu is used due to the fact that Mn is a stronger β stabiliser. The sintering conditions used ensure complete chemical homogeneity and the precipitation of the Ti_2Cu intermetallic phase via the eutectoid reaction when Cu is added as an alloying element. Independently of their chemistry, the quaternary Ti alloys are characterised by an elastic + plastic deformation behaviour. The resistance to plastic deformation increases and the ability to withstand plastic deformation decreases when the amount of alloying elements is increased. Due to their finer lamellar microstructure, the Mn-bearing quaternary Ti alloys are stronger and harder but more brittle with respect to their Cu-bearing counterparts. This transforms the fracture surface from rough and composed of dimples to smoot with faceted fractured areas. The quaternary Ti alloys share the same work hardening behaviour due to their lamellar microstructure but the rapid or progressive decrement of the curves is alloy dependent as dictated by the coarseness of the microstructure which also determines the ability to undergo plastic deformation once necking occurred. Generally, the quaternary Ti alloys have higher ultimate tensile strength with similar or lower hardness to comparable alloys.

CRediT authorship contribution statement

M. Al-hajiri: Methodology, Investigation. **F. Yang:** Methodology. **L. Bolzoni:** Writing – review & editing, Methodology, Investigation,

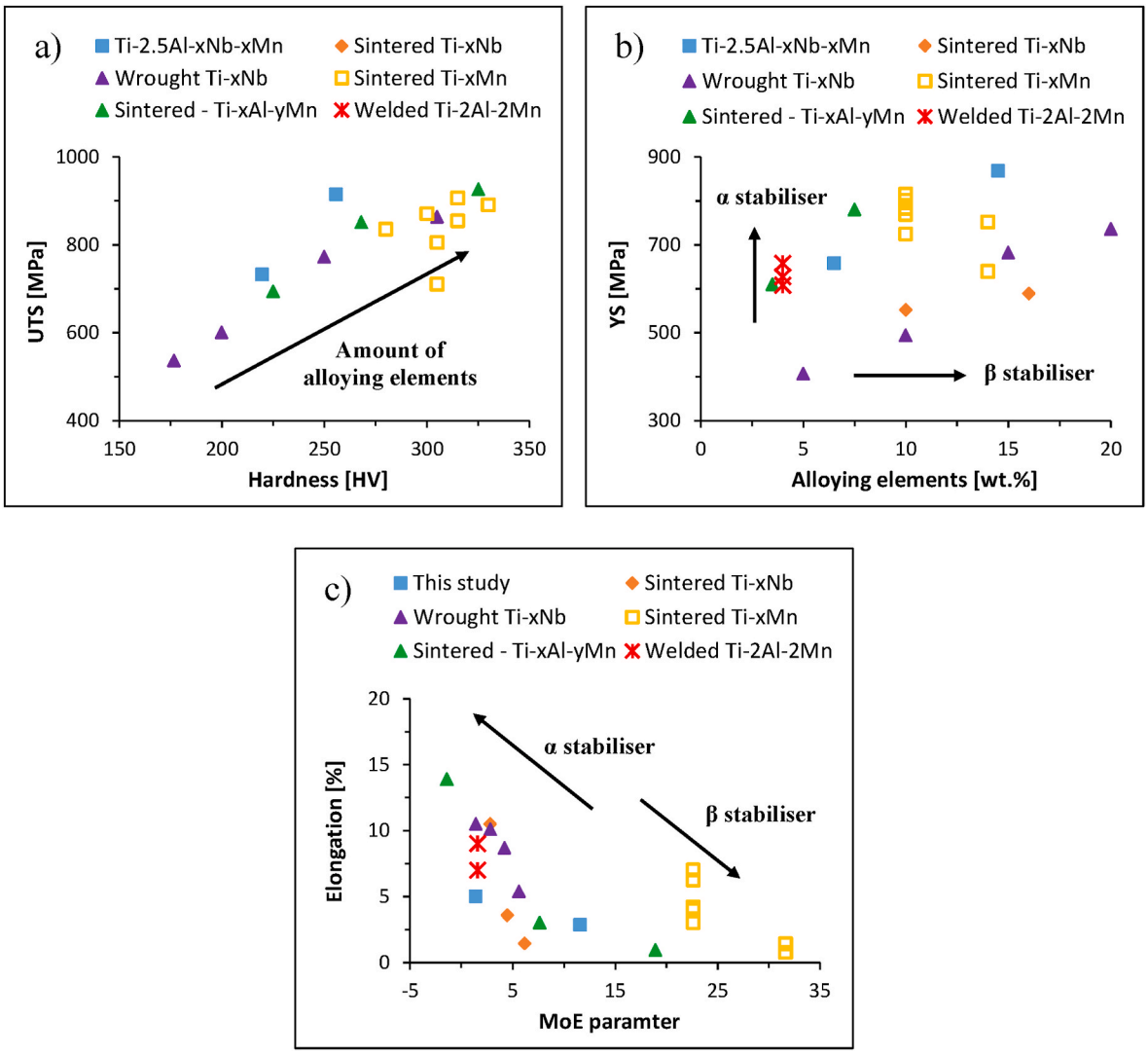

Fig. 13. Comparison of the mechanical properties of the quaternary Ti-2.5Al-xNb-xMn alloys with literature [17,28,58,61,62]: a) UTS versus hardness, b) YS versus total amount of alloying elements, and c) elongation at fracture versus MoE parameter.

Conceptualization.

Declaration of competing interest

The authors declare no conflict of interest.

Data availability

Data will be made available on request.

Acknowledgements

This research did not receive any specific grant from funding agencies in the public, commercial, or not-for-profit sectors.

References

[1] L. Bolzoni, M. Xia, N. Hari Babu, Formation of equiaxed crystal structures in directionally solidified Al-Si alloys using Nb-based heterogeneous nuclei, Sci. Rep. 6 (1) (2016) 39554.
[2] G. Szczęsny, M. Kopec, D.J. Politis, Z.L. Kowalewski, A. Łazarski, T. Szolc, A review on biomaterials for orthopaedic surgery and traumatology: from past to present, Materials 15 (10) (2022) 3622.
[3] A. Amherd Hidalgo, R. Frykholm, T. Ebel, F. Pyczak, Powder metallurgy strategies to improve properties and processing of titanium alloys: a review, Adv. Eng. Mater. 19 (6) (2017) 1600743.
[4] L. Bolzoni, M. Paul, F. Yang, Effect of combined lean additions of isomorphous and eutectoid beta stabilisers on the properties of titanium, J. Mater. Res. Technol. 21 (2022) 3828–3843.
[5] X. Zhou, H. Fang, T. Yuan, R. Li, Effect of slight Sn modification on mechanical properties and corrosion behavior of Ti- (2-4 wt%) Mn alloys fabricated via powder metallurgy, Mater. Char. 203 (2023) 113068.
[6] H. Zhang, C. Wang, F. Pyczak, T. Ebel, X. Liu, A new kind of biomedical Ti-Mn-Nb alloy, Phys. Status Solidi 220 (7) (2023) 2200348.
[7] S. Raynova, Y. Collas, F. Yang, L. Bolzoni, Advancement in the pressureless sintering of CP titanium using high-frequency induction heating, Metall. Mater. Trans. 50 (10) (2019) 4732–4742.
[8] J. Lu, P. Ge, Y. Zhao, Recent development of effect mechanism of alloying elements in titanium alloy design, Rare Met. Mater. Eng. 43 (4) (2014) 775–779.
[9] Q. Li, Q. Huang, J.-j. Li, Q.-F. He, M. Nakai, K. Zhang, M. Niinomi, K. Yamanaka, A. Chiba, T. Nakano, Microstructure and mechanical properties of Ti-Nb-Fe-Zr alloys with high strength and low elastic modulus, Trans. Nonferrous Metals Soc. China 32 (2) (2022) 503–512.
[10] L. Raganya, N. Moshokoa, B. Obadele, E. Makhatha, R. Machaka, Microstructure and mechanical properties of Ti-Mo-Nb alloys designed using the cluster-plus-glue-atom model for orthopedic applications, Int. J. Adv. Des. Manuf. Technol. 115 (9) (2021) 3053–3064.
[11] P. Qi, B. Li, T. Wang, L. Zhou, Z. Nie, Microstructure and properties of a novel ternary Ti-6Zr-xFe alloy for biomedical applications, J. Alloys Compd. 854 (2021) 157119.
[12] M.-K. Han, J.-Y. Kim, M.-J. Hwang, H.-J. Song, Y.-J. Park, Effect of Nb on the microstructure, mechanical properties, corrosion behavior, and cytotoxicity of Ti-Nb alloys, Materials 8 (9) (2015) 5986–6003.

[13] C.M. Lee, C.P. Ju, J.H. Chern Lin, Structure-property relationship of cast Ti-Nb alloys, J. Oral Rehabil. 29 (4) (2002) 314–322.
[14] L.-J. Xu, S.-l. Xiao, J. Tian, Y.-y. Chen, Y.-d. Huang, Microstructure and dry wear properties of Ti-Nb alloys for dental prostheses, Trans. Nonferrous Metals Soc. China 19 (2009) s639–s644.
[15] M. Kikuchi, M. Takahashi, O. Okuno, Mechanical properties and grindability of dental cast Ti-Nb alloys, Dent. Mater. J. 22 (3) (2003) 328–342.
[16] Y. Bai, Y. Deng, Y. Zheng, Y. Li, R. Zhang, Y. Lv, Q. Zhao, S. Wei, Characterization, corrosion behavior, cellular response and in vivo bone tissue compatibility of titanium–niobium alloy with low young's modulus, Mater. Sci. Eng. C 59 (2016) 565–576.
[17] D. Zhao, K. Chang, T. Ebel, M. Qian, R. Willumeit, M. Yan, F. Pyczak, Microstructure and mechanical behavior of metal injection molded Ti-Nb binary alloys as biomedical material, J. Mech. Behav. Biomed. Mater. 28 (2013) 171–182.
[18] E. Yılmaz, A. Gökçe, F. Findik, H.O. Gulsoy, Metallurgical properties and biomimetic HA deposition performance of Ti-Nb PIM alloys, J. Alloys Compd. 746 (2018) 301–313.
[19] D. Kalita, Ł. Rogal, T. Czeppe, A. Wójcik, A. Kolano-Burian, P. Zackiewicz, B. Kania, J. Dutkiewicz, Microstructure and mechanical properties of Ti-Nb alloys prepared by mechanical alloying and Spark Plasma sintering, J. Mater. Eng. Perform. 29 (3) (2020) 1445–1452.
[20] E. Eisenbarth, D. Velten, M. Muller, R. Thull, J. Breme, Biocompatibility of β-stabilizing elements of titanium alloys, Biomaterials 25 (26) (2004) 5705–5713.
[21] M. Kikuchi, Y. Takada, S. Kiyosue, M. Yoda, M. Woldu, Z. Cai, O. Okuno, T. Okabe, Mechanical properties and microstructures of cast Ti-Cu alloys, Dent. Mater. 19 (3) (2003) 174–181.
[22] E. Zhang, X. Wang, M. Chen, B. Hou, Effect of the existing form of Cu element on the mechanical properties, bio-corrosion and antibacterial properties of Ti-Cu alloys for biomedical application, Mater. Sci. Eng. C 69 (2016) 1210–1221.
[23] C.B. Yi, Z.Y. Ke, L. Zhang, J. Tan, Y.H. Jiang, Z.Y. He, Antibacterial Ti-Cu alloy with enhanced mechanical properties as implant applications, Mater. Res. Express 7 (10) (2020) 105404.
[24] E. Zhang, J. Ren, S. Li, L. Yang, G. Qin, Optimization of mechanical properties, biocorrosion properties and antibacterial properties of as-cast Ti-Cu alloys, Biomed. Mater. 11 (6) (2016) 065001.
[25] E. Zhang, S. Li, J. Ren, L. Zhang, Y. Han, Effect of extrusion processing on the microstructure, mechanical properties, biocorrosion properties and antibacterial properties of Ti-Cu sintered alloys, Mater. Sci. Eng. C 69 (2016) 760–768.
[26] J. Liu, F. Li, C. Liu, H. Wang, B. Ren, K. Yang, E. Zhang, Effect of Cu content on the antibacterial activity of titanium-copper sintered alloys, Mater. Sci. Eng. C 35 (2014) 392–400.
[27] M.K. Gouda, K. Nakamura, M.A.H. Gepreel, Effect of Mn-content on the deformation behavior of binary Ti-Mn alloys, Key Eng. Mater. 705 (2016) 214–218.
[28] K. Cho, M. Niinomi, M. Nakai, J. Hieda, P. Fernandes Santos, Y. Itoh, M. Ikeda, Mechanical properties, microstructures, and biocompatibility of low-cost β-type Ti-Mn alloys for biomedical applications, Biomater. Sci.: Processing, Properties and Applications IV 251 (2014) 21–30.
[29] L. Strause, P. Saltman, J. Glowacki, The effect of deficiencies of manganese and copper on osteoinduction and on resorption of bone particles in rats, Calcif. Tissue Int. 41 (3) (1987) 145–150.
[30] H. Sigel, Metal ions in biological systems: volume 37, in: Manganese and its Role in Biological Processes Metal Ions in Biological Systems, CRC Press, 2000.
[31] J.-W. Kim, M.-J. Hwang, M.-K. Han, Y.-G. Kim, H.-J. Song, Y.-J. Park, Effect of manganese on the microstructure, mechanical properties and corrosion behavior of titanium alloys, Mater. Chem. Phys. 180 (2016) 341–348.
[32] P. Fernandes Santos, M. Niinomi, H. Liu, K. Cho, M. Nakai, Y. Itoh, T. Narushima, M. Ikeda, Fabrication of low-cost beta-type Ti-Mn alloys for biomedical applications by metal injection molding process and their mechanical properties, J. Mech. Behav. Biomed. Mater. 59 (2016) 497–507.
[33] Y. Alshammari, M. Jia, F. Yang, L. Bolzoni, The effect of α+ β forging on the mechanical properties and microstructure of binary titanium alloys produced via a cost-effective powder metallurgy route, Mater. Sci. Eng., A 769 (2020) 138496.
[34] L.A. Matlakhova, A.N. Matlakhov, S.N. Monteiro, S.G. Fedotov, B.A. Goncharenko, Properties and structural characteristics of Ti-Nb-Al alloys, Mater. Sci. Eng., A 393 (1) (2005) 320–326.
[35] M. Koike, T. Okabe, Properties characterization of cast Ti-Al-Cu alloys for dental applications, medical device materials IV, in: Proceedings from the Materials and Processesfor Medical Devices Conference 2007, 2007, pp. 109–113.
[36] E.-S.M. Sherif, H.S. Abdo, F.H. Latief, N.H. Alharthi, S.Z.E. Abedin, Fabrication of Ti-Al-Cu new alloys by inductive sintering, characterization, and corrosion evaluation, J. Mater. Res. Technol. 8 (5) (2019) 4302–4311.
[37] L. Blacha, B. Oleksiak, A. Smalcerz, T. Matuła, Changes in Ti-Al-Mn alloy compositions during their smelting in a vacuum induction furnace, Archives of Materials Science and Engineering 58 (1) (2012) 28–32.
[38] A.V. Mikhaylovskaya, A.O. Mosleh, A.D. Kotov, J.S. Kwame, T. Pourcelot, I. S. Golovin, V.K. Portnoy, Superplastic deformation behaviour and microstructure evolution of near-α Ti-Al-Mn alloy, Mater. Sci. Eng., A 708 (2017) 469–477.
[39] M. Takahashi, M. Kikuchi, Y. Takada, Mechanical properties and microstructures of dental cast Ti-6Nb-4Cu, Ti-18Nb-2Cu, and Ti-24Nb-1Cu alloys, Dent. Mater. J. 35 (4) (2016) 564–570.
[40] I. Mutlu, E. Oktay, Localised corrosion behaviour of biomedical implant materials using electrochemical potentiokinetic reactivation and critical pitting potential methods, corrosion engineering, Sci. Technol. 50 (1) (2015) 72–79.
[41] Z. Chen, Y. Liu, H. Jiang, M. Liu, C.H. Wang, G.H. Cao, Microstructures and mechanical properties of Mn modified, Ti-Nb-based alloys, J. Alloys Compd. 723 (2017) 1091–1097.
[42] S. Ehtemam-Haghighi, H. Attar, M.S. Dargusch, D. Kent, Microstructure, phase composition and mechanical properties of new, low cost Ti-Mn-Nb alloys for biomedical applications, J. Alloys Compd. 787 (2019) 570–577.
[43] L. Bolzoni, M. Alqattan, L. Peters, Y. Alshammari, F. Yang, Ternary Ti alloys functionalised with antibacterial activity, Sci. Rep. 10 (1) (2020) 22201.
[44] M. Alqattan, L. Peters, Y. Alshammari, F. Yang, L. Bolzoni, Antibacterial Ti-Mn-Cu alloys for biomedical applications, Regenerative Biomaterials 8 (1) (2020) rbaa050.
[45] H. Wang, Z.Z. Fang, P. Sun, A critical review of mechanical properties of powder metallurgy titanium, Int. J. Powder Metall. 46 (5) (2010) 45–57.
[46] T. Sjafrizal, A. Dehghan-Manshadi, D. Kent, M. Yan, M.S. Dargusch, Effect of Fe addition on properties of Ti-6Al-xFe manufactured by blended elemental process, J. Mech. Behav. Biomed. Mater. 102 (2020) 103518.
[47] M. Morinaga, Alloy design based on molecular orbital method, Mater. Trans. 57 (3) (2016) 213–226.
[48] P.J. Bania, Beta titanium alloys and their role in the titanium industry, JOM 46 (7) (1994) 16–19.
[49] Q. Wang, C. Dong, P.K. Liaw, Structural stabilities of β-Ti alloys studied using a new Mo equivalent derived from [β/(α + β)] phase-boundary slopes, Metall. Mater. Trans. 46 (8) (2015) 3440–3447.
[50] J.D. Cotton, R.D. Briggs, R.R. Boyer, S. Tamirisakandala, P. Russo, N. Shchetnikov, J.C. Fanning, State of the art in beta titanium alloys for airframe applications, JOM 67 (6) (2015) 1281–1303.
[51] L. Bolzoni, E.M. Ruiz-Navas, E. Gordo, Powder metallurgy CP-Ti performances: hydride-dehydride vs. sponge, Mater. Des. 60 (2014) 226–232.
[52] P.G. Esteban, E.M. Ruiz-Navas, E. Gordo, Influence of Fe content and particle size on the processing and mechanical properties of low-cost Ti-xFe alloys, Mater. Sci. Eng., A 527 (21) (2010) 5664–5669.
[53] F. Zhang, A. Weidmann, B.J. Nebe, E. Burkel, Preparation of TiMn alloy by mechanical alloying and Spark Plasma sintering for biomedical applications, J. Phys. Conf. 144 (1) (2009) 012007.
[54] J.L. Murray, Phase Diagrams of Binary Titanium Alloys, first ed., ASM International, 1987.
[55] M.T. Jia, B. Gabbitas, L. Bolzoni, Evaluation of reactive induction sintering as a manufacturing route for blended elemental Ti-5Al-2.5Fe alloy, J. Mater. Process. Technol. 255 (2018) 611–620.
[56] U.F. Kocks, H. Mecking, Physics and phenomenology of strain hardening: the FCC case, Prog. Mater. Sci. 48 (3) (2003) 171–273.
[57] L. Weber, M. Kouzeli, C. San Marchi, A. Mortensen, On the use of considere's criterion in tensile testing of materials which accumulate internal damage, Scripta Mater. 41 (5) (1999) 549–551.
[58] Y. Zhang, D. Sun, J. Cheng, J.K.H. Tsoi, J. Chen, Mechanical and biological properties of Ti-(0-25 wt%)Nb alloys for biomedical implants application, Regenerative Biomaterials 7 (1) (2020) 119–127.
[59] L. Bolzoni, F. Yang, Development of Cu-bearing powder metallurgy Ti alloys for biomedical applications, J. Mech. Behav. Biomed. Mater. 97 (2019) 41–48.
[60] Y. Alshammari, F. Yang, L. Bolzoni, Fabrication and characterisation of low-cost powder metallurgy Ti-xCu-2.5Al alloys produced for biomedical applications, J. Mech. Behav. Biomed. Mater. 126 (2022) 105022.
[61] Y. Alshammari, S. Mendoza, F. Yang, L. Bolzoni, Effect of Mn on the properties of powder metallurgy Ti-2.5Al-xMn alloys, Materials 16 (14) (2023) 4917.
[62] K.K. Murthy, S. Sundaresan, Effect of microstructural features on the fracture toughness of a welded alpha-beta Ti-Al-Mn alloy, Eng. Fract. Mech. 58 (I/2) (1997) 29–41.